Design Feature Sensitivity Analysis in a Numerical Model of an Extrusion Spider Die

A. G. Mamalis,[1] G. Kouzilos,[2] A. K. Vortselas[2]

[1]*Project Center for Nanotechnology and Advanced Engineering, National Center of Scientific Research "Demokritos," 15310 Agia Paraskevi, Athens, Greece*
[2]*Laboratory of Manufacturing Technology, National Technical University of Athens, 9 Iroon Polytechniou str., 15870, Athens, Greece*

Received 28 April 2011; accepted 28 April 2011
DOI 10.1002/app.34762
Published online 10 August 2011 in Wiley Online Library (wileyonlinelibrary.com).

ABSTRACT: In this work, we aimed to develop an optimum design for a spider die used for the extrusion of high-density polyethylene tubes. For this purpose, a computational-fluid-dynamics-based model using the generalized Newtonian approach was employed to investigate the pressure drop, flow, and temperature uniformity in the die. © 2011 Wiley Periodicals, Inc. J Appl Polym Sci 122: 3537–3543, 2011

Key words: computer modeling; extrusion; polyethylene (PE)

INTRODUCTION

The production of extruded polyethylene films, rods, tubes, and pipes is a common industrial process that has been the subject of major investigations over many years.[1–3] The majority of plastic tubes and components for fluid transport and other industrial applications are mainly manufactured by polymer extrusion with an annular inline or straight-through die. What is most important in the design of such a die is to secure the inner mandrel of the die to its external casing by means of ties (spider legs). In polymer extrusion processes, product quality is affected by the homogeneity of the flow speed and the temperature at the die exit. Inhomogeneity causes shape distortions and material weak spots (weld lines). The major cause for such inhomogeneity in spider dies is the discontinuity and distortion caused to the flow by the spider legs [Fig.1(c)], whereas the die sections aft of the spider work to rehomogenize the flow. The weld lines result not only in variations in the wall thickness of the pipe but, more importantly, in a region of reduced mechanical properties in the extruded pipe. One of the important mechanical properties of a polymer is its fatigue life. It may give rise to premature brittle or ductile failure, even at surprisingly low loads, usually well below the yield stress.[4,5]

The homogeneity is vital because an unbalanced flow produces a distorted product having residual stresses.[4,5] Complex cross sections, flow properties of polymeric melts (e.g., viscoelasticity), and operating conditions, such as temperature and speed, could further complicate the die design procedure.[6] Except for some simple shapes, such as circular dies, it is very difficult to design a die that can properly operate over a wide range of operating conditions and for various polymers.[7] For most companies, obtaining the final shape of an extruded product is a time-consuming trial-and-error process. It can take a few trials to get the correct die cut that will yield the desired part shape and dimensions. The cost of the preliminary tests and corrections of a profile die may be as much as 10–50% of the total cost.[8] Meeting the current and anticipated growth in demand of complex extruded shapes requires quick and accurate die design from the start. Ideally, the design of the die will minimize the process of trial and error and avoid costly shutdown of production lines. Computer simulation (science) using computational fluid dynamics (CFD) can supplement existing experience (art) in the die design process by providing a cost-effective tool to investigate new design options. Moreover, coupling computational modeling with existing in-house experience facilitates the transfer of knowledge to the entire die design team and increases the range of possibilities for innovative approaches. The new tools can handle nonlinear behavior, nonisothermal flow, and different rheological models of molten plastic. Even if the flow behavior is modeled accurately, it does not necessarily entail that the final computational results will have the same accuracy. This is because phenomena such as extrudate swelling, draw down, and cooling strongly affect the shape and size of the final product.

Correspondence to: A. G. Mamalis (mamalis@ims.demokritos.gr).

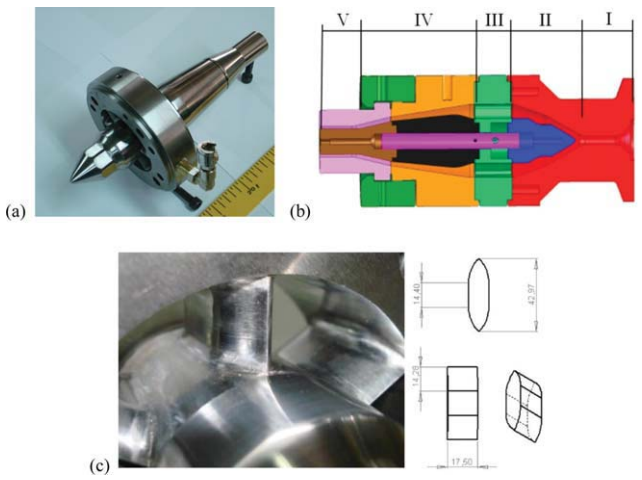

Figure 1 (a) Core mandrel and spider assembly, (b) spider die zones, and (c) detail and dimensions of reference geometry spider legs. [Color figure can be viewed in the online issue, which is available at wileyonlinelibrary.com.]

In almost all cases, a numerical analysis coupled with an optimization process is applied in the design of a profile die.[9–16] A number of numerical methods have been developed and adopted for the simulation of non-Newtonian flow, including the finite difference method, the finite element method (FEM), the finite volume method, and the boundary element method. Among them, FEM is widely applied for the investigation of complex flow problems because of its excellent adaptability to complex geometric boundaries.[17]

The optimization algorithm must be carefully chosen when one single analysis using three-dimensional software requires several hours of CPU time. Nondeterministic or stochastic methods, such as the Monte Carlo method and genetic algorithms,[15] can obtain a global minimum, but they need a lot of evaluations for the functions to converge. Gradient methods[18,19] require the computations of the gradients of the functions; the computation of gradients by finite difference is time consuming and depends on the perturbed parameters. For these reasons, we decided to chose a response surface method (RSM).[20] Often, the number of the involved variables and their interactions prevent any optimization according to the trial-and-error corrections because the number of evaluations needed may become very high. The design of an experiment, in particular, the Taguchi method,[21] allows one to obtain invaluable information about the important variables of the process to achieve the required goals.

In this work, we aimed to develop an optimum design for a spider die used for the extrusion of high-density polyethylene (HDPE) tubes. For this purpose, a CFD-based model using the generalized Newtonian approach was employed to investigate the pressure drop, flow, and temperature uniformity in the die. CFD-based approaches have been developed previously by other researchers to study various aspects of flow in extrusion dies.[9–16,22,23] The numerical calculations for the three-dimensional flow and temperature fields were performed with a finite-element-based CFD code Comsol 3.5. The ultimate goal of this work was to optimize the spider die geometry in such a way that a uniform velocity distribution was obtained at the die exit.

EXPERIMENTAL

The spider die was manufactured with IMPAX (tool steel), which was selected for its high strength and wear resistance. It is important to note that this material cannot be easily machined, so electrodischarge machining has to be used; this is a factor that has to be considered in the optimization of the geometry of the die design.

- Zone I constituted the fluid entrance zone in the die.
- Zone II was the area where the fluid diverted from the extrusion axis was distributed through the mandrel cone into a ring-shaped cross section.
- Zone III was the spider zone, in which one end of the die (male) was constrained by the spider legs [Fig.1(b)].
- Zone IV was the relaxation zone, where the flow marks generated by the spider legs could be extinguished and lead, in this way, to a uniform flow.
- Zone V was the final stage before the extrusion product exited the die; in this zone, the pipe took its final dimensions and shape.

Because the spider die was intended to be used for the production of HDPE tubes, it was mounted on a single-screw Johnson Plastics extruder with the following characteristics: length/diameter ratio = 24 : 1, screw diameter = 38 mm, and compression ratio = 2.75. An HDPE tube with an external diameter of 32 mm and a wall thickness of 2.4 mm was produced with the aforementioned equipment.

Material properties

The material used in the extrusion experiments was HDPE type SABIC B 5823. Some of the most important characteristics of the material, such as melt flow rate (MFR), strain rate, and viscosity, are presented in Tables I and II.

Because the material properties greatly affect the analysis of the entire processing operation, the use of reliable models is essential. However, in many

TABLE I
Density and MFR of HDPE

Polymer properties	Units/SI	B5823	Test method
MFR			ISO 1133
At 190°C, 2.16 kg	dg/min	0.16	
At 190°C, 5 kg	dg/min	0.89	
At 190°C, 21.6 kg	dg/min	23	
Density	kg/m^3	958	ISO 1183

polymer processes, the elastic memory effects are not very important because the melts are subjected to large steady rates of deformation for a relatively long period of time.[8] Because this work was concentrated on a qualitative analysis of the flow regimes, the inelastic model was selected. Polymer melts are non-Newtonian fluids. The viscosity–shear rate dependence of non-Newtonian liquids is typically represented by one of several viscosity models and is referred to as *viscosity*.[24] Various models exist for describing the dependence of viscosity (η) on the shear rate and temperature. A great deal of flexibility is provided by the Carreau–Yasuda model:

$$\text{Carreau} - \text{Yasuda model}: \quad \eta = a_T\eta_0(T_R)\{1 + [a_T\dot{\lambda}(T_R)\dot{\gamma}]^a\}^{(n-1)/a} \quad (1)$$

$$\text{Shift factor}: \quad a_T = \exp[E_0/R(1/T_R - 1/T)] \quad (2)$$

where, in the Carreau–Yasuda model, η_0, λ, a and n are the fitting parameters and T_R is reference temperature for material properties. More specifically, η_0 denotes the viscosity at a shear rate of zero, λ is the time constant with its reciprocal representing the shear rate at the transition from Newtonian to shear-thinning behavior, a determines the width of the transition region, and n is the power-law index describing the slope of the viscosity curve with respect to the shear rate in the shear-thinning region. The temperature dependence in the Carreau–Yasuda model is introduced in Eq. (2) through a_T, where E_0 is the activation energy and R is the universal gas constant. The shear viscosity and shear rate dependence of the polymer is presented in Figure 2. The parameters used in the Carreau–Yasuda model are given in Table III.

The temperature dependence of the physical properties of HDPE are given in Table IV as polynomials

TABLE II
Viscosity Measurements of HDPE at 190°C

Shear rate (1/s) at 190°C	Viscosity (Pa·s)
12	4770
23	3426
58	1991
115	1301
230	836
565	443
1135	224

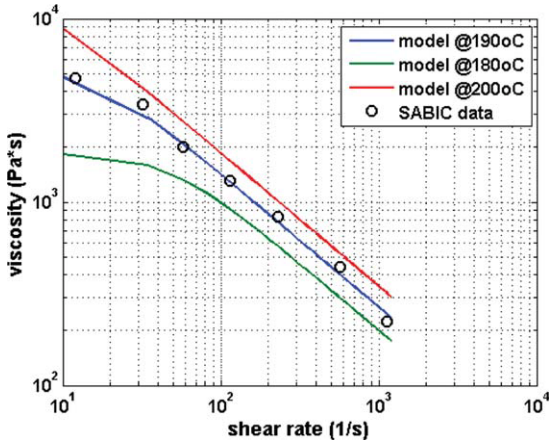

Figure 2 Recorded viscosities of HDPE at 180, 190, and 200°C and their fits according to the Carreau–Yasuda and Power law models. [Color figure can be viewed in the online issue, which is available at wileyonlinelibrary.com.]

in the form $A + BT + CT^2$, where T is the temperature in degrees centigrade.[25]

Numerical modeling

In this study, a three-dimensional conjugate heat-transfer model was developed for non-Newtonian materials processed in the extrusion die. The numerical solution assumes that a homogeneous and isotropic HDPE melt with a uniform temperature of 469 K is flowing into the spider die. The temperature of the die wall is kept at a constant value (T_w = 469 K), and the volumetric flow rate of the melt is fixed at $\dot{V}_{max} = 7.9 \times 10^{-6}$ m^3/s.

According to the theory of CFD, the governing equations to solve the melt flow problems can be obtained from the continuity equation, motion equation, and energy equation, respectively, on the basis of the conservation of mass, momentum, and energy.[26] Considering the characteristics of the polymer melt flow in the die channel when a steady extrusion is arrived, we made the following assumptions:

1. Incompressible, steady laminar flow. The variation of the system physical variables versus time could be neglected when a steady extrusion process was arrived.
2. The melt flow velocity at the fluid die/mold interface was equal to the moving velocity of the die wall.

TABLE III
Carreau Model Constants

Model parameters	
n	0.2723
η_0	5.43×10^3 Pa s
λ	0.063 s
E_0	6.5 kcal/mol
T_R	190°C
A	2

TABLE IV
Temperature Dependence of the Physical Properties of HDPE

Physical property	Polymer type	Temperature (°C)	A	B
k (W/m K)	HDPE	143–200	0.26	—
C_p (kJ kg^{-1} K^{-1})	HDPE	133–200	1.984	$3.88\cdot\times 10^{-3}$
ρ^{-1} (cm^3/g)	HDPE	133–200	1.158	$8.09\cdot\times 10^{-4}$

3. The inertial and gravitational forces were not considered. The Reynolds number of the polymer melt was low; therefore, the effects of the inertial and gravitational forces were negligible.

On the basis of these assumptions, the governing equations could be written as follows:

$$\text{Continuity equation} : \nabla \mathbf{u} = 0 \tag{3}$$

$$\text{Motion equation} : \nabla \sigma = 0 \tag{4}$$

$$\text{Energy equation} : \ \rho C_p \mathbf{u} \nabla T = -\nabla q + Q \tag{5}$$

where ∇ is the Hamilton differential operator; ρ is the material density; C_p is the heat capacity; T is the temperature; k is the thermal conductivity; Q (heat flux) is the total source term, incorporating the streamline-upwind Petrov–Galerkin scheme, which was employed to improve the computation stability; $\mathbf{u}$ is the velocity vector; and σ is the Cauchy stress tensor, which is expressed as follows:

$$\sigma = -pI + \mathbf{S} \tag{6}$$

where p is the hydrostatic pressure, $\mathbf{S}$ is the extra stress tensor, and I is the Kronecker operator.

The governing equations were solved numerically with finite element CFD code, Comsol 3.5. The numerical solution included the Carreau–Yasuda model. In this case, the problem considered was the viscous dissipation, which caused an increase of the fluid temperature. The shape of the simulated domain was derived from the die design with a streamlined process, which is detailed later (Fig. 6).

Figure 3(a) shows the pressure distributions in the entire domain of the die, as calculated by the finite element simulation for the reference geometry. The pressure decreased continuously from the die inlet to the outlet, for a total pressure drop of 10 MPa; this was validated by experimental results. The axial thrust load on the die core was 3.04–3.36 kN. The viscosity dropped at high-velocity zones but remained above 5000 Pa s in the spider section. The flow was decelerated at the spider zone because of the higher cross section; then, it was accelerated and homogenized in the relaxation and end zones. The calculated increase in the melt temperature, due to viscous dissipation, was only 2° above the uniform 469°K of the die walls.

FORMULATION OF THE OPTIMIZATION PROBLEM

Objective and constraint functions

The Taguchi method can determine the experimental condition having the least variability as the optimum condition. The variability of a property is due to a noise factor, which is difficult to control, and can be expressed by the signal-to-noise ratio (SNR) measured in decibels. The experimental condition having the maximum SNR is considered as the optimum condition, as the variability of characteristics is inversely proportional to the SNR.

Our optimization problem consists in determining an optimal geometry to homogenize the velocity distribution through the die exit, which corresponds to the minimum of the velocity dispersion. The inhomogeneity of flow velocity distribution is often addressed as the variability in a velocity measurement experiment and, as such, can be described by an SNR, see similar work in ref. [27]. Hence, the SNR for flow velocity at the nodes of the melt exit cross section was chosen as the objective function for homogeneity (max is better):

$$\text{SNR} = 10 \times \log_{10}\left(\frac{\bar{X}^b}{s}\right)^2 \tag{7}$$

where $\overline{X}$ and s are the mean and standard deviation of velocities and b is derived from the least-squares

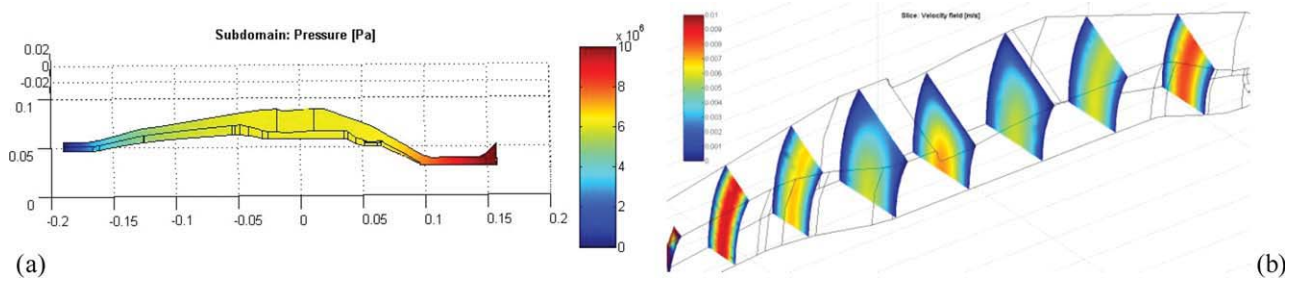

Figure 3 (a) Pressure distribution and (b) velocity distribution at various cross sections around the spider leg. [Color figure can be viewed in the online issue, which is available at wileyonlinelibrary.com.]

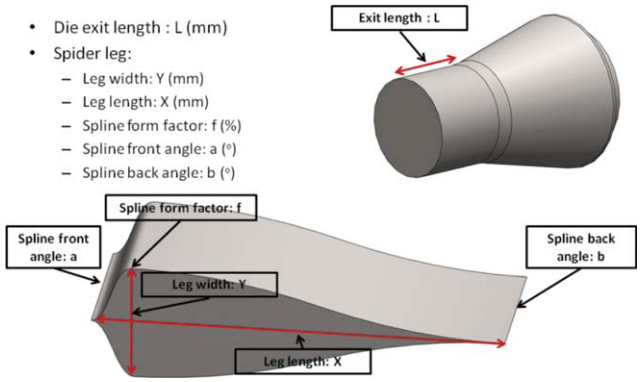

Figure 4 Optimization parameters. [Color figure can be viewed in the online issue, which is available at wileyonlinelibrary.com.]

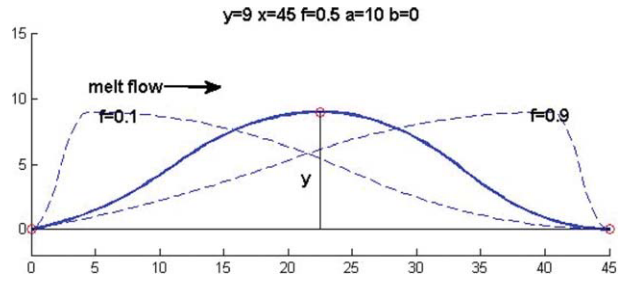

Figure 5 Effect of f on the shape of the spider leg cross section to be optimized. [Color figure can be viewed in the online issue, which is available at wileyonlinelibrary.com.]

regression: $\log_{10}(s_i) = a + b \log_{10}(\overline{X}_i)$.[28] In our case, we find $b = 1$, with a very high R value. Furthermore, temperature inhomogeneity was found to be insignificant in all cases (SNR $\approx$ 60), so only velocity was used for the objective function.

Design variables

Five geometric characteristics of the spider leg cross section (Y, X, f, a, and b), plus the length of the die exit zone (L; Fig. 4), were selected for sensitivity analysis and optimization, to help us determine the areas where modifying the die design would be most effective. The variable L represents the exit length of the spider die (Zone V), the variable Y represents the leg width, X represents the spider leg length, the variable f represents spline form factor [Fig. 5(a)] and the variables a and b represent the spline front and back angles, respectively. Each variable has its geometrical limitations which are, respectively, $24 \leq L \leq 45$ mm, $9 \leq Y \leq 12$ mm, $30 \leq X \leq 80$ mm, $0.1 \leq f \leq 0.9$, $0^\circ \leq a \leq 15^\circ$, $0^\circ \leq b \leq 15^\circ$. Initially, the geometrical variables of the die are $L = 45$ mm, $Y = 12$ mm, $X = 43$ mm, f = 0.5, $a = b = 30^\circ$.

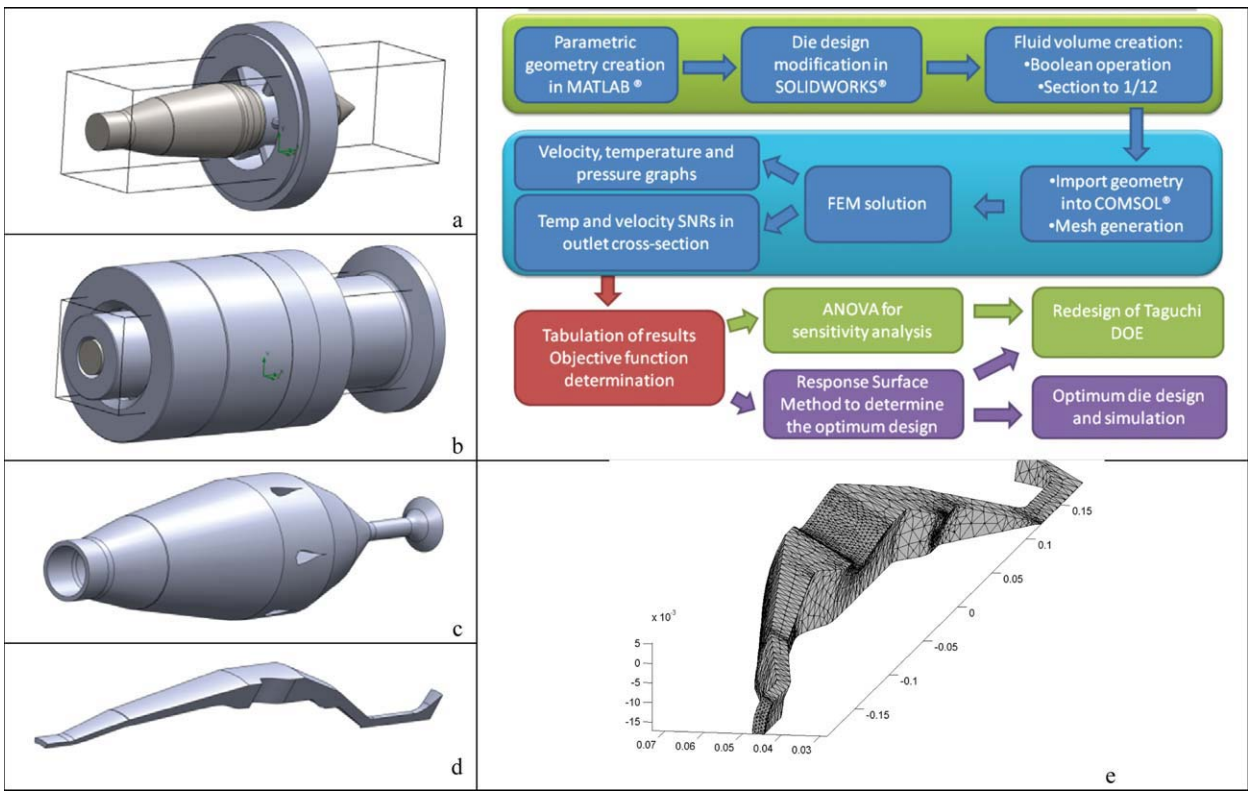

Figure 6 Optimization process flowchart and consecutive design steps: (a) core mandrel and spider assembly, (b) assembly of the whole die, (c) melt volume, (d) 1/12 of the melt volume, and (e) adaptive meshing of the melt volume. [Color figure can be viewed in the online issue, which is available at wileyonlinelibrary.com.]

TABLE V
Optimization Parameters and Design of Experiments (DOE) Levels

Parameter		Level 1	Level 2	Level 3
L	Exit length (mm)	24	34.5	45
Y	Leg width (mm)	9	10.5	12
X	Spider leg length (mm)	30	55	80
F	Spline form factor	0.1	0.5	0.9
A	Spline front angle (°)	0	5	10
B	Spline back angle (°)	0	5	10

OPTIMIZATION PROCEDURE AND RESULTS

For each set of design variables that we wish to examine, the respective spline curve is created (Fig.5) and used to modify the geometry of the spider part in a computer aided design (CAD) environment [Fig. 6 (a,b)]. The fluid volume is extracted from the die assembly [Fig. 6(c)] and 1/12 of it is meshed [taking advantage of symmetry planes; Fig.6(d)] and imported in the FEM environment [Fig.6(e)], where the problem is solved. Postprocessing of the solution involves sampling of velocity and temperature at the die exit cross section and calculation of the objective function, based on the mean and standard deviation of the two sampled parameters at the sampling points. The results of the objective function are tabulated. Analysis of variance (ANOVA) is employed for sensitivity analysis and the quadratic RSM is employed to find the position of the optimum point inside the design space.

All the above steps are scripted in a programming environment, as illustrated in the flowchart of Figure 6. This level of streamlining is crucial for the practicality of such an optimization technique, because it performs the required number of simulations with time restrictions imposed only by the run time of the finite element solver (up to 10 min each on a PC).

For the optimization task presented here, three levels were selected for each parameter, with design limitations taken into consideration, and an initial Taguchi design of experiments was drafted, for a total of 27 experiments (Table V).

Velocity SNR values ranged between 6 for the reference geometry die and 7.52 for the optimum point (Table VI). ANOVA results indicate that the effect of *L* was overwhelming, and more importantly, contradicted the empirical choice of a high length for zone V. Of the other parameters, only *X* had a significant effect.

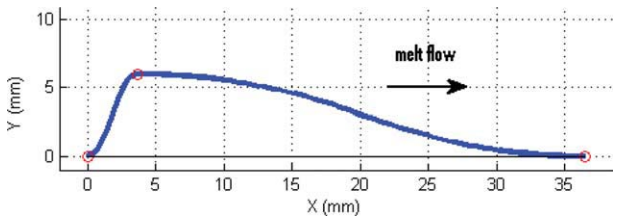

Figure 7 Spline curve for the optimum spider leg cross section, as detailed in Table VI. [Color figure can be viewed in the online issue, which is available at wileyonlinelibrary.com.]

A second Taguchi experiment, with five parameters ($L = 24$ mm was finalized), three levels, and 36 points was conducted. Now, the effect of *X* was overwhelming, and $X = 30$ mm was finalized. Subsequent optimization runs, where *L* and *X* were constants, led to the determination of optimum points for *Y*, *f*, *a*, and *b*, but because their effect was insignificant, these steps could be omitted (Table VI).

The optimum spider leg design (Fig. 7) seemed to be the one that provided the best streamlining of the flow aft of the maximum leg thickness point, while keeping the die length at a minimum. Because the flow was laminar, the flow velocity profile downstream of the spider was chiefly affected by shearing viscosity. This was the ultimate reason for the overwhelming effect of both *L* and *X*.

CONCLUSIONS

A non-Newtonian CFD model of the spider die polymer extrusion process, correlating well with experimental results, was created. A streamlined design process, enabling the optimization of die design features, was implemented. A sensitivity analysis and optimization procedure, performed on the effects of six design parameters on the flow homogeneity, was used to validate the design choices and pinpoint the features for which further optimization would be feasible.

This procedure demonstrated that *L* and *X* had overwhelming effects and had to be minimized,

TABLE VI
Determination of the Optimum (Opt) Point for the Examined Sampling Methods with Quadratic RSM

		L27_6		L36_5		L36_4		L9_2	
	Parameter	Opt	ANOVA	Opt	ANOVA	Opt	ANOVA	Opt	ANOVA
L	Exit length (mm)	24	82%	24	—	24	—	24	—
Y	Leg width (mm)	9.0	1.6%	9.0	2.20%	9.0	27.84%	9	—
X	Spider leg length (mm)	30.0	12.60%	30	85.90%	30	—	30	—
f	Spline form factor	0.10	1.9%	0.36	3.76%	0.20	30.02%	0.20	—
a	Spline front angle (°)	10.0	0.5%	5.0	4.17%	5.0	27.66%	5.0	54.31%
b	Spline back angle (°)	0.0	0.1%	5.0	3.97%	5.0	14.48%	5.0	45.69%

whereas the other parameters were of lesser importance, and their design optimization had to be balanced against the manufacturing simplicity of the spider part. The spline angles *a* and *b* could be chosen at will without any practical effect on the flow homogeneity.

References

1. Yan, H.; Xia, J. Sci Tech Adv Mater 2006, 7, 127.
2. Ding, F.; Giacomin, A. J. Polym Eng Sci 2004, 44, 1811.
3. Krishnaswamy, R. K.; Rohlfing, D. C.; Sukhadi, A. M.; Slusarz, K. R. Polym Eng Sci 2004, 44, 2266.
4. Soury, E.; Behravesh, A. H.; Ghasemi, H.; Zolfaghari, A. J Reinforc Plast Compos 2010, 50, 543.
5. Nobrega, J. M.; Carneiro, O. S.; Oliviera, P. J.; Pinho, F. T. Presented at the 18th Annual Conference of the Polymer Processing Society, PPS-18, Guimaraes, Portugal, Jun 2002.
6. Ettinger, H. J.; Sienz, J.; Pittman, J. F. T. Struct Multidisc Optim 2004, 27, 1.
7. Rauwendaal, C. Polymer Extrusion; Hanser: Munich, 2001.
8. Michaeli, W. Extrusion Dies for Plastics and Rubber; Hanser: Munich, 1992.
9. Yu, Y. W.; Liu, T. J. J Polym Res 1998, 5, 1.
10. Xiaorong, Y.; Changyu, S.; Chuntai, L.; Lixia, W. Chin J Comput Mech 2004, 21, 253.
11. Puissant, S.; Demay, Y.; Vergnes, B. Polym Eng Sci 1994, 34, 201.
12. Smith, D. E.; Tortorelliav, D. A.; Tucker, C. L. Comput Methods Appl Mech Eng 1998, 167, 283.
13. Michaeli, W.; Kaul, S.; Wolff, T. J Polym Eng 2001, 21, 225.
14. Sun, Y.; Gupta, M. Soc Plast Eng Annu Tech Conf Technical Pap 2004, 3307.
15. Michaeli, W.; Kaul, S. J Polym Eng 2004, 24, 123.
16. Ettinger, H. J.; Sienz, J.; Pittman, J. F. T.; Polynkin, A. Struct Multidisc Optim 2004, 28, 180.
17. Gao, X. W. Int J Numer Methods Fluids 2005, 47, 19.
18. Smith, D. E.; Tortorelliav, D. A.; Tucker, C. L. Comput Methods Appl Mech Eng 1998, 167, 303.
19. Hurez, P.; Tanguy, P. A.; Blouin, D. Polym Eng Sci 1996, 36, 626.
20. Lebaal, N.; Puissant, S.; Schmidt, F. M. J Mater Process Tech Papers 2005, 34, 1524.
21. Montgomery, D. C. Design and Analysis of Experiments; Wiley: Hoboken, 2005.
22. Zhang, M.; Sun, S.; Jia, Y. Polym-Plast Technol Eng 2008, 47, 384.
23. Mamalis, A. G.; Spentzas, K. N.; Kouzilos, G.; Theodorakopoulos, I.; Pantelelis, N. G. J Adv Polym Technol 2010, 29, 172.
24. Macosko, C. W. Rheology: Principles, Measurements, and Applications; Wiley-VCH: New York, 1994.
25. Baird, D.; Collias, D. Polymer Processing—Principles and Design; Wiley: New York, 1998.
26. Nassehi, V. Practical Aspects of Finite Element Modelling of Polymer Processing; Wiley: England, 2002.
27. Kwan, C. T.; Jan, F. S.; Lee, W. C. J Mater Processing Technol 2008, 201, 145.
28. Logothetis, N. Appl Stat 1990, 39, 31.